Published online 12 September 2014 *Nucleic Acids Research, 2014, Vol. 42, No. 18* ***11697–11706***
doi: 10.1093/nar/gku820

Dynamics of RNA modification by a multi-site-specific tRNA methyltransferase

Djemel Hamdane[1,2,*], Amandine Guelorget[1], Vincent Guérineau[3] and Béatrice Golinelli-Pimpaneau[1,2,*]

[1]Laboratoire d'Enzymologie et Biochimie Structurales, Centre de Recherche de Gif, CNRS, 1 avenue de la Terrasse, 91198 Gif-sur-Yvette, France, [2]Laboratoire de Chimie des Processus Biologiques, Collège de France, CNRS, 11 place Marcelin Berthelot, 75231 Paris Cedex 05, France and [3]Institut de Chimie des Substances Naturelles, Centre de Recherche de Gif, CNRS, 1 avenue de la Terrasse, 91198 Gif-sur-Yvette, France

Received June 10, 2014; Revised August 26, 2014; Accepted August 29, 2014

ABSTRACT

In most organisms, the widely conserved 1-methyladenosine58 (m^1A_{58}) tRNA modification is catalyzed by an S-adenosyl-L-methionine (SAM)-dependent, site-specific enzyme TrmI. In archaea, TrmI also methylates the adjacent adenine 57, m^1A_{57} being an obligatory intermediate of 1-methyl-inosine57 formation. To study this multi-site specificity, we used three oligoribonucleotide substrates of *Pyrococcus abyssi* TrmI ($_{Pab}$TrmI) containing a fluorescent 2-aminopurine (2-AP) at the two target positions and followed the RNA binding kinetics and methylation reactions by stopped-flow and mass spectrometry. $_{Pab}$TrmI did not modify 2-AP but methylated the adjacent target adenine. 2-AP seriously impaired the methylation of A_{57} but not A_{58}, confirming that $_{Pab}$TrmI methylates efficiently the first adenine of the $A_{57}A_{58}A_{59}$ sequence. $_{Pab}$TrmI binding provoked a rapid increase of fluorescence, attributed to base unstacking in the environment of 2-AP. Then, a slow decrease was observed only with 2-AP at position 57 and SAM, suggesting that m^1A_{58} formation triggers RNA release. A model of the protein–tRNA complex shows both target adenines in proximity of SAM and emphasizes no major tRNA conformational change except base flipping during the reaction. The solvent accessibility of the SAM pocket is not affected by the tRNA, thereby enabling S-adenosyl-L-homocysteine to be replaced by SAM without prior release of monomethylated tRNA.

INTRODUCTION

Modified nucleosides are abundant and of wide chemical diversity in transfer RNAs (tRNAs). They influence translation accuracy, reading frame maintenance, recognition by aminoacyl-tRNA synthetases and tRNA structure (1–3). The modifications found in RNAs occur post-transcriptionally and range from simple base or ribose methylations to more complex multi-step reactions (4). Most RNA modifying enzymes are mono-site specific, introducing a chemical group at a specific position in a target nucleotide. Nonetheless, there are a few RNA modifying enzymes that display a regional multi-site specificity, modifying consecutive positions in RNA. For instance, *Aquifex aeolicus* tRNA (*N*2,*N*2-guanine)-dimethyltransferase Trm1 catalyzes the methylation not only of guanine 26 but also guanine 27 in tRNA (5,6). In *Escherichia coli,* the pseudouridine synthase TruA specifically modifies uridines at positions 38, 39 and/or 40 in the anticodon stem loop of tRNAs (7), while rRNA MTase KsgA catalyzes the dimethylation at the N6 position of two adjacent adenines A1518 and A1519 in the small subunit of ribosomal RNA (8,9). Although the multisite specificities of these enzymes have been pointed out, no detailed mechanistic studies have yet been reported. Most of these enzymes have their structures solved but not their complexes with RNA or the RNA was in an unproductive conformation (10). When the structures in complex with RNA are known (7), they reveal the molecular features of the stabilization of the flipped base, but are less informative about the binding, base recognition and flipping processes.

The bi-specific tRNA adenine-N1, A_{57}-A_{58}-methyltransferase (MTase), named TrmI, from the archaeum *Pyrococcus abyssi* ($_{Pab}$TrmI) methylates two adjacent adenines in tRNA (11). $_{Pab}$TrmI catalyzes the transfer of a methyl group from S-adenosyl-L-methionine (SAM) to nitrogen 1 of A_{57} and the adjacent A_{58} in the

*To whom correspondence should be addressed. Tel: 33 1 44 27 12 52; Fax: 33 11 44 27 13 56; E-mail: beatrice.golinelli@college-de-france.fr
Correspondence may also be addressed to Djemel Hamdane. Tel: 33 1 44 27 16 45; Fax: 33 1 44 27 13 56; E-mail: djemel.hamdane@college-de-france.fr

T-loop of tRNAs. In contrast to m^1A_{58}, a conserved modification found in all organisms and shown to be essential for cell growth in yeast (12) and for adaptation to high temperatures in thermophilic organisms (13), m^1A_{57} is exclusively encountered in archaea as a precursor of 1-methylinosine (m^1I) at position 57 (14,15). In particular, the presence of m^1A together with that of m^1I was detected after incubation of a $tRNA^{Ile}$ transcript with *Haloferax volcanii* extracts (14), despite the fact that m^1A_{58} has never been found in any of the 51 tRNAs of this species sequenced so far, and these two modified nucleotides were not detected with a transcript in which A_{57} was mutated to G_{57}. Therefore, it was attested that, *in vivo,* the formation of m^1A_{57} catalyzed by a SAM-dependent MTase is followed by the deamination of the 6-amino group of the adenine moiety by a currently unknown deaminase to produce m^1I_{57}.

In general, the multi-site specificity mechanism of these enzymes is not yet well understood. In the case of $_{Pab}$TrmI, we have proposed that the enzyme recognizes the presence of three consecutive adenines ($A_{57}A_{58}A_{59}$) in *P. abyssi* tRNAs. Indeed, A_{58} is methylated by $_{Pab}$TrmI only if an adenine is present at position 59, suggesting that the enzyme methylates the first adenine of an AA sequence (16). Moreover, mass spectrometry (MS) analysis of methylated $_{Pab}tRNA^{Asp}$ formed by $_{Pab}$TrmI indicated the presence of monomethylated A_{57}, in addition to the dimethylated product, but not that of monomethylated A_{58}, suggesting that the enzyme modifies sequentially A_{57} and then A_{58}. This implies the existence of an RNA binding pocket with a large specificity for the nucleotide to be modified (to accommodate A or m^1A) and a rather strict one for the following nucleotide (adenine). Crystal structures of TrmIs from several organisms have been determined (17,18) but the structures in complex with RNA are still missing. Yet, the structure of TrmI from *Thermus thermophilus* solved in complex with S-adenosyl-L-homocysteine (SAH) revealed an active site binding pocket suited to bind a flipped-out adenine, suggesting that the enzyme uses a base flipping mechanism (19). Indeed, RNA modification enzymes commonly introduce such a structural change inside the tRNA to make the nucleoside accessible for modification (20,21). Typically, the enzyme flips the nucleobase to be modified, removing its internal stacking and hydrogen bonding interactions, to expose it to the protein active site.

The most commonly employed method for studying these local nucleotide conformational changes in solution is to replace the target base by 2-aminopurine (2-AP), a fluorescent nucleotide analog (Supplementary Figure S1). The ease, sensitivity and specificity of 2-AP fluorescence detection make the use of 2-AP very attractive. 2-AP is commonly used to probe nucleic acid structure in loops because it rarely affects structure adversely, and its fluorescence is typically enhanced when its environment is disturbed as a result of decreased stacking interactions (22). Therefore, 2-AP is an excellent probe to follow the conformational changes of the target base itself or its neighbors. Indeed, when 2-AP is stacked between DNA bases, its fluorescence is strongly quenched, but the fluorescence increases and shifts when 2-AP adopts a flipped-out position (23,24). This fluorescent analog has also been substituted to nucleobases in strategic positions of single-stranded RNA molecules to act as a probe to monitor folding and folding dynamics of RNAs in a few cases (25–28).

We applied this spectroscopic method relying on the 2-AP fluorescence to study the RNA conformational changes occurring during modification by $_{Pab}$TrmI. A57 and A58 are located in the T-loop of tRNA. A58 is involved in a reverse Hoogsteen base pair interaction with U54 within the loop and is more buried inside the tRNA than A57, which is not base-paired. The difference between A and 2-AP is the removal of the amino group at position 6 and addition of an amino group at position 2 (Supplementary Figure S1). Thus, 2-AP retains the same base-pairing capacities as adenine but with a different geometry. By replacing A_{57} or A_{58} with 2-AP and by following the fluorescence changes during the methylation reaction, we gained deeper insight into the mechanism of $_{Pab}$TrmI. In addition, we built a structural model of $_{Pab}$TrmI in complex with a tRNA, which enabled us to provide a model of the sequence of events along the dual base modification.

MATERIALS AND METHODS

Material

The 2-AP containing RNAs were ordered from Thermo Fisher Scientific Dharmacon. Prior to reaction, they were refolded by heating at 80°C for 5 min, and then cooling on ice for 2 min.

Purification of $_{Pab}$TrmI

The recombinant *P. abyssi* PAB0283 protein ($_{Pab}$TrmI) bearing a C-terminal His-tag was expressed as described previously (11). After lysis, the cells supernatant was loaded onto a Nickel-NTA affinity column (5 ml; Qiagen) pre-equilibrated in 50 mM Tris-HCl pH 8.5, 500 mM KCl and eluted with the same buffer containing 200 mM imidazole. The sample was then loaded onto a Superdex 200 HR 10/30 column (GE healthcare Inc.) equilibrated in Tris-HCl, 500 mM KCl, 200 mM imidazole. The fractions containing the protein were pooled and concentrated with a Vivaspin concentrator (10 kDa PES membrane; Sartorius).

Mass spectrometry analysis

The mini-RNA (20 μM) was incubated for 1 h at 60°C with 10 μM of purified wild-type $_{Pab}$TrmI and 1 mM SAM in 50 μl 50 mM Tris-HCl pH 8, 10 mM $MgCl_2$. The reaction was stopped with 200 μl of phenol:chloroform:isoamylic alcohol (25:24:1) pH 4.5 to precipitate the protein. tRNA in the aqueous phase was extracted by centrifugation at 10 000 g for 5 min, ethanol precipitated and desalted on a MicroSpin G-25 column (GE Healthcare). One microgram of desalted tRNA was then digested at 37°C overnight in 10 μl of 50 mM DHB (2,5-dihydroxybenzoic acid; Sigma-Aldrich, Saint Quentin Fallavier, France) containing 2 μg of RNase A (Fermentas). One microliter of digest was mixed with 9 μl DHB (20 mg/ml in water: methanol 50:50) and 1 μl of the mixture was spotted on the MALDI plate and air-dried

('dried droplet' method). MALDI-TOF MS and MALDI-TOF/TOF MS/MS analyses were performed directly on the digestion products using a 4800 MALDI TOF/TOF Analyzer mass spectrometer (ABSciex, Les Ulis, France). The instrument is equipped with an Nd:YAG laser (operating at 355 nm wavelength of <500 ps pulse and 200 Hz repetition rate). Acquisitions were performed in positive ion mode except those for determining the methylation kinetics that were measured in negative ion mode to ensure that the positive charge generated on the N1 atom of adenine upon m^1A formation does not affect ionization and that the percentage of methylated RNA can be accurately quantified by measuring the area of the peaks corresponding to the non-methylated and methylated fragments. For MS/MS experiments, precursor ions were accelerated at 8 kV and the MS/MS spectra were acquired using 1 kV collision energy with CID gas (argon) at a pressure of 3.5×10^{-6} Torr. MS data were processed using DataExplorer 4.4 (Applied Biosystems).

Steady-state fluorescence assay

The emission fluorescence spectra of 2-AP containing mini-RNAs alone and in complex with $_{Pab}$TrmI were recorded in a quartz cuvette at 37°C on a Cary eclipse fluorescence spectrophotometer (Varian). The excitation and emission slits were set at 5 and 10 nm, respectively. After exciting at 320 nm, the fluorescence emission was recorded every nm from 335 to 550 nm. The resulting spectra were corrected from the contribution of the buffer (50 mM Tris-HCl pH 8.0, 10 mM $MgCl_2$). In all experiments, the concentration of RNA was 0.5 μM while that of $_{Pab}$TrmI was varied. Before recording the spectra, enzyme and RNA were incubated for 5 min to reach the equilibrium.

Stopped-flow kinetics

The experiments were performed on a TGK Scientific SF-61DX2 stopped-flow fluorescence spectrophotometer equipped with a temperature-controlled circulating water bath. RNA (1 μM) was rapidly mixed with $_{Pab}$TrmI (6 μM) alone or in complex with SAM (1 mM) or SAH (1 mM). All reactions were performed in reaction buffer (50 mM Tris-HCl pH 8.0, 10 mM $MgCl_2$) at various temperatures. Before rapid mixing, the samples loaded in the stopped flow syringes were incubated for 10 min at the appropriate temperature. 2-AP fluorescence was recorded by exciting at 320 nm and collecting through a WG-360 nm cut-off filter. Up to five transients were collected and averaged for each condition. Background signal was determined against buffer to allow data scaling. The observed rates (k_i) were determined by fitting the averaged transients to multiple exponentials equation using the SigmaPlot 12 software. The temperature dependence of each k_i was measured and the energies of activation (E_a) were determined using the following equation: $k_i = A^*\exp(-E_{ai}/RT)$.

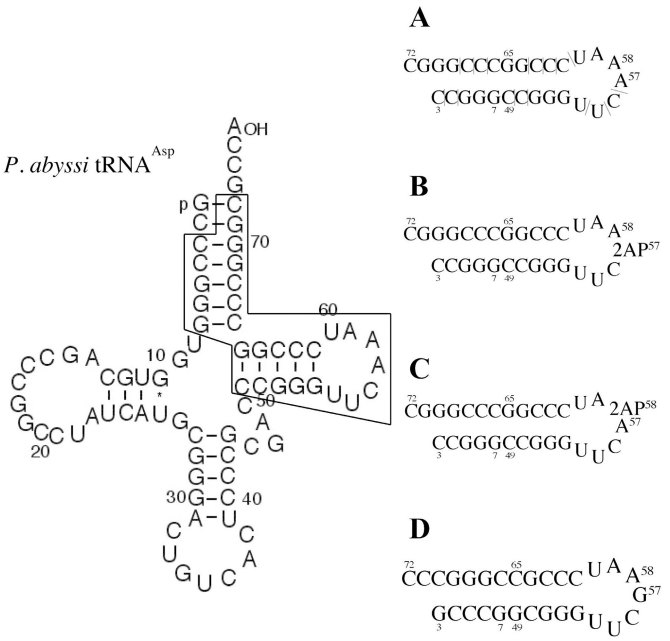

Figure 1. Sequence and secondary structure of the mini-RNAs tested for the methylation and binding studies of $_{Pab}$TrmI. (**A**) mini-tRNA^{Asp}. The fragments obtained after RNase A treatment are indicated by a dash. (**B**) 2AP57: mini-tRNA^{Asp} containing 2-AP at position 57 instead of A_{57}. (**C**) 2AP58: mini tRNA^{Asp} containing 2-AP at position 58 instead of A_{58}. (**D**) mini-tRNA^{Arg}.

RESULTS

$_{Pab}$TrmI recognizes and methylates both A57 and A58 in mini-tRNA^{Asp} containing the $A_{57}A_{58}A_{59}U_{60}$ sequence

We have previously shown that $_{Pab}$TrmI recognizes and methylates the first adenine of an AA sequence in a full-length tRNA (16). While $_{Pab}$TrmI methylates both A_{57} and A_{58} in tRNA^{Asp}, it becomes mono-site specific with the *P. abyssi* A_{59}G tRNA^{Asp} mutant, A_{57} being the only targeted base. To verify if the tertiary tRNA L-shaped structure is required for the multi-site specificity, we tested whether $_{Pab}$TrmI methylates a 29-mer *P. abyssi* mini-tRNA^{Asp}, which includes the acceptor stem and the T-arm of *P. abyssi* tRNA^{Asp} (Figure 1A). Indeed, several RNA-modification enzymes recognize a stem-loop, in which they can efficiently extrude and modify the targeted base. We used MS to examine if the methylation has occurred and to identify the modified positions. After incubation with the enzyme and SAM, the mini-RNA was digested by RNase A, which cleaves after C and U and generates 3′-phosphate nucleosides, and its fragments were analyzed by MALDI MS (Supplementary Figure S2) (29). When incubated with $_{Pab}$TrmI, the spectrum of digested mini-tRNA^{Asp} showed fragments at m/z 1326.15 and 1340.17 (Supplementary Figure S2A) coinciding with the expected masses of mono and dimethylated fragments derived from AAAUp, corresponding to the sequence from A_{57} to U_{60} in mini-tRNA^{Asp} (Figure 1A). The positions of the modifications at the nucleotide level were then identified by tandem mass spectrometry (MS/MS) analysis (Supplementary Figure S2B). In this technique, individual oligonucleotides of interest, which have been previ-

ously identified by standard MALDI-MS analysis, are isolated and subjected to controlled fragmentation (29). The sequence of the dimethylated fragment obtained after incubation with $_{Pab}$TrmI (Supplementary Figure S2B) was determined to be m^1Am^1AAUp, indicating that both adenines at positions 57 and 58 in mini-tRNA^{Asp} are methylated. Indeed, the presence of the z2 fragment, corresponding to the AUp sequence (m/z 636.10), combined with the absence of the z2 + m fragment, corresponding to the m^1AUp sequence, shows that A_{59} is not methylated. Moreover, the presence of the c2 fragment corresponding to the m^1Am^1Ap sequence (m/z 687.14) confirms that both A_{57} and A_{58} are methylated.

$_{Pab}$TrmI recognizes and methylates only A58 in mini-tRNA^{Arg} (TCT) containing the $G_{57}A_{58}A_{59}U_{60}$ sequence

Interestingly, all 43 tRNAs from *P. abyssi* contain either the $A_{57}A_{58}A_{59}$ or $G_{57}A_{58}A_{59}$ sequence. To confirm that $_{Pab}$TrmI methylates the first adenine of an AA sequence inside the T-loop of tRNA (16), we tested the *P. abyssi* mini-tRNA^{Arg} (TCT), which possesses the $G_{57}A_{58}A_{59}U_{60}$ sequence (Figure 1D), as a substrate of $_{Pab}$TrmI. As confirmed by MS and MS/MS analysis (Supplementary Table S1), only A_{58} is methylated by $_{Pab}$TrmI in mini-tRNA^{Arg}.

The 2-AP replacing the target adenines in a mini-RNA substrate is not methylated by $_{Pab}$TrmI

The *P. abyssi* mini-tRNAs^{Asp} containing 2-AP either at position 57 or 58 (named as 2AP57 and 2AP58) were incubated with $_{Pab}$TrmI and SAM, digested by RNase A and the resulting fragments were analyzed by MALDI MS (Supplementary Figure S3). When the adenine at position 57 was replaced by 2-AP (2AP57; Figure 1B), the mini-RNA was methylated by $_{Pab}$TrmI at a unique site, as evidenced by the presence of a + 14 Da fragment (1326.07 Da compared to 1312.21 for the control experiment) (Supplementary Figure S3A). MS/MS analysis of the digested RNA identified A_{58} as being the methylation site and indicated that the 2-AP at position 57 was not methylated by $_{Pab}$TrmI (Supplementary Figure S3B). Interestingly, A_{58} was almost completely modified, as indicated by the very small intensity of the non-methylated fragment (Supplementary Figure S3A). Similarly, when the adenine at position 58 of *P. abyssi* mini-tRNA^{Asp} was replaced by a 2-AP (2AP58; Figure 1C), $_{Pab}$TrmI methylated only A_{57} (Supplementary Figure S3C and D). However, the methylation of A_{57} was not as efficient as that of A_{58} in 2AP57, as demonstrated by the large amount of non-methylated fragment.

The methylation of A_{58} is not impaired by 2-AP at the adjacent position 57

To further confirm the more efficient methylation of A_{58} in a 2-AP-containing mini-RNA substrate, the kinetics of m^1A_{57} and m^1A_{58} formation were followed at 60°C with MS. While 2AP57 was methylated too fast by $_{Pab}$TrmI for measuring an accurate rate constant by MS, the time course of methylation of 2AP58 by $_{Pab}$TrmI yielded an observed rate constant for methylation of A_{57} of 0.05 min^{-1} (Figure 2). This clearly indicates a more efficient methylation of A_{58} than A_{57} in the 2-AP-containing mini-RNAs.

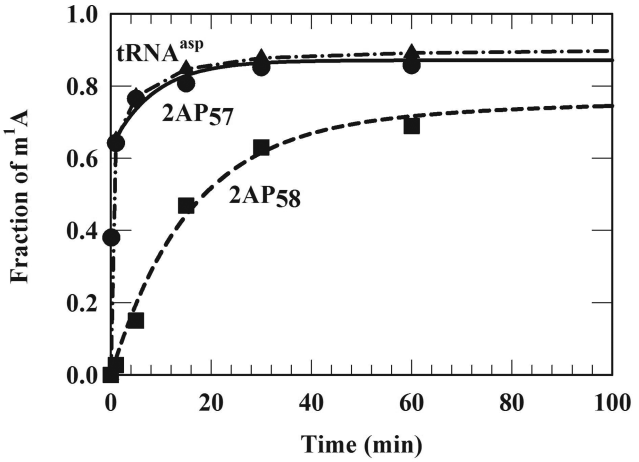

Figure 2. Methylation kinetics of tRNA^{Asp}, 2AP57 and 2AP58 by $_{Pab}$TrmI. An equimolar amount of appropriate RNA (tRNA^{Asp}, triangles; 2AP58 squares; 2AP57 closed circles) and enzyme (20 μM) was incubated in the presence of SAM at 60°C for different incubation times. The reaction was stopped and the modified RNA was then digested with RNase. The digest was analyzed by MALDI mass spectrometry in negative ion mode. The area of the peaks corresponding to the monomethylated fragment (2-AP)m^1AAUp at m/z 1324.07 or m1A(2-AP)AUp at m/z 1324.18 was compared to that of the peaks corresponding to the non-methylated (m/z 1310.21) fragment to obtain the percentage of monomethylated tRNA. For the full-length tRNA, the area of the peak corresponding to the dimethylated fragment m1Am1AAUp at m/z 1338.22 was compared to that of the peaks corresponding to the non-methylated (m/z 1310.19) and monomethylated (m/z 1324.20) fragments to obtain the percentage of dimethylated tRNA.

Moreover, the methylation kinetics of 2AP57 were very similar to those of the full-length *P. abyssi* tRNA^{Asp} (Figure 2).

Interaction of 2-AP-containing mini-RNAs with $_{Pab}$TrmI

To know if the interaction of $_{Pab}$TrmI with a 2-AP-containing mini-RNA substrate modifies the target base environment, we followed the fluorescence emission spectra from 340 to 460 nm after exciting at 320 nm 2AP57 and 2AP58 in the presence of enzyme (Figure 3). Because the fluorescence from the protein is negligible under our experimental conditions, the observed variation of fluorescence can be exclusively attributed to a change of the 2-AP environment. In the absence of enzyme, both 2AP57 and 2AP58 fluoresce with a maximum peak at ∼373 nm. Addition of a 7-fold molar excess of $_{Pab}$TrmI to either 2AP57 or 2AP58 resulted in 91% and 43% fluorescence increase, respectively. This increase of fluorescence is associated with a small blue shift of the maximum peak indicating a polarity change in the 2-AP environment. The 2-AP-mini-RNA fluorescence change with increasing concentrations of $_{Pab}$TrmI shows a hyperbolic shape in agreement with a binding event (Figure 3C). The apparent dissociation constants of 2AP57 and 2AP58 for $_{Pab}$TrmI deduced from this experiment were 1.7 and 2.8 μM, respectively.

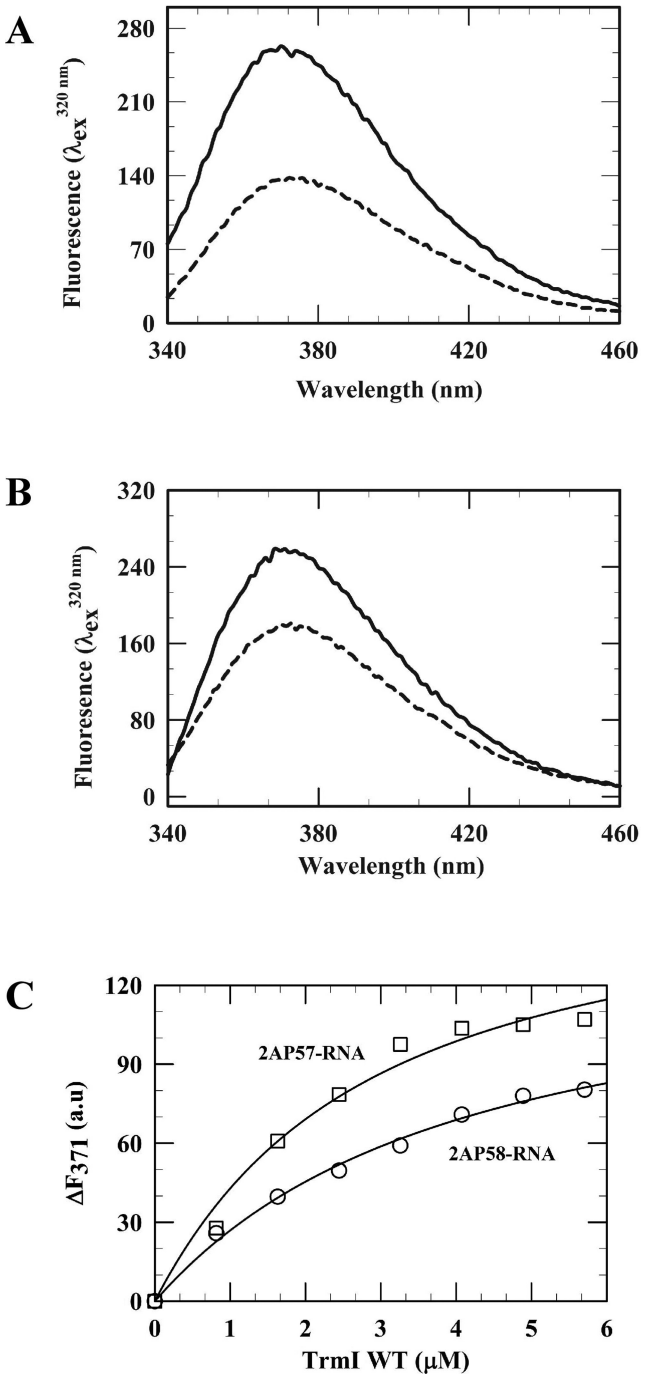

Figure 3. Emission fluorescence spectra of 2AP57 (**A**) and 2AP58 (**B**) in the absence (dash lines) and presence of $_{Pab}$TrmI (solid lines). The concentration of RNA was 0.5 μM and that of $_{Pab}$TrmI was 6.5 μM. (**C**) Fluorescence titration of the 2-AP containing mini-RNAs with $_{Pab}$TrmI. Increasing amounts of enzyme were incubated with 0.5μM 2-AP-mini-RNA in 50 mM Tris-HCl pH 8.0, 10 mM $MgCl_2$ at 37°C for 5 min before monitoring the emission fluorescence spectrum (λ_{exc} = 320 nm).

Dynamics of RNA binding by $_{Pab}$TrmI in the absence of methyl donor

To further investigate the dynamics of RNA binding to $_{Pab}$TrmI, the pre-steady-state kinetics of 2-AP fluorescence increase at λ_{ex} = 320 nm after the rapid mixing of either

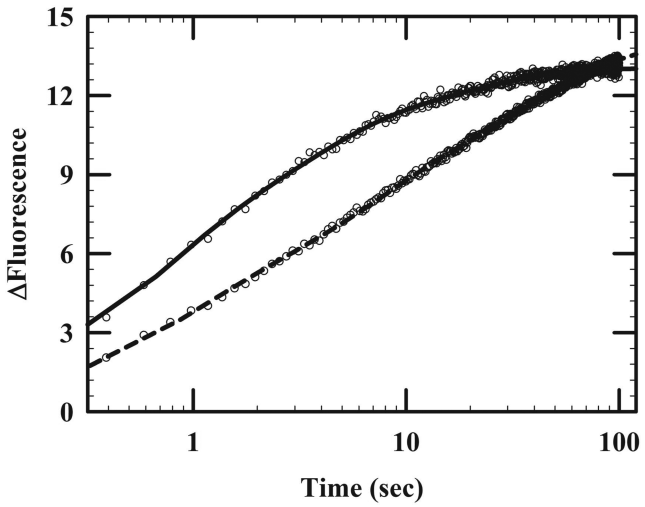

Figure 4. Base destacking kinetics of the 2-AP containing mini-RNAs by $_{Pab}$TrmI in the absence of SAM at 37°C measured with a stopped-flow spectrofluorimeter. After the rapid mixing of the $_{Pab}$TrmI (1 μM) from one syringe with either 2AP57 or 2AP58 (1 μM) from another syringe, the total fluorescence was recorded with a WG-360 cut-off filter after exciting at 320 nm. The experimental data points are shown as circles while the simulation curves are in solid and dashed lines for 2AP57 and 2AP58, respectively. The kinetics were best fitted with three exponentials.

2AP57 or 2AP58 with an excess of free enzyme in the absence of SAM were monitored by stopped flow in fluorescence mode. When 1 μM 2AP57 or 2AP58 was mixed with 6 μM $_{Pab}$TrmI, an increase in the fluorescence emission of the 2-AP-containing RNAs was observed within a second (Figure 4), followed by several slower processes. The kinetics of 2AP57 and 2AP58 binding by $_{Pab}$TrmI were best fitted with three exponentials (Table 1). The binding of 2AP57 by $_{Pab}$TrmI was slightly faster than that of 2AP58 (k_1 and k_3 of 2AP57 are, respectively, 1.4 and 2.5 times faster than those of 2AP58), in agreement with a better affinity of the enzyme for 2AP57.

Dynamics of RNA binding by $_{Pab}$TrmI in the presence of SAM

To get further insights into the recognition mechanism of A_{57} and A_{58} under catalytic conditions, $_{Pab}$TrmI was premixed with a saturated concentration of SAM, the methyl donor, before mixing with the 2-AP-mini-RNAs. Importantly, the addition of SAM to the 2-AP-mini-RNAs did not affect the fluorescence level of 2-AP (Supplementary Figure S4). The kinetics were recorded after excitation at 320 nm as aforementioned (Table 2 and Figure 5). Remarkably, not only the shapes of the kinetics curves were different from those observed in the absence of SAM but they also differed markedly between 2AP57 and 2AP58 (Figure 5A and B).

In the case of 2AP57, the kinetics were best fitted to three exponentials, a biphasic exponential increase of fluorescence during the first 5 s (7.62 s^{-1} and 1.1 s^{-1}) being followed by a decrease with a rate constant of 0.12 s^{-1} (Table 2 and Figure 5A).

In the case of 2AP58, the kinetics were also triphasic (rate constants of 2.8 s^{-1}, 0.6 s^{-1} and 0.13 s^{-1}) but less complex, with a steady increase of fluorescence until a plateau was

Table 1. Amplitudes and observed rate constants for the base destacking kinetics of 2AP57, 2AP58 by $_{Pab}$TrmI in the absence of cofactor

	A_1	A_2 (%)	A_3	k_1	k_2 (s^{-1})	k_3
2AP57	43	39	18	1.8	0.34	0.05
2AP58	28	32	40	1.3	0.2	0.02

Table 2. Amplitudes and observed rate constants for the base destacking kinetics of 2AP57, 2AP58 and G57-2AP58-miniRNA by $_{Pab}$TrmI in the presence of SAM or SAH

	A_1	A_2 (%)	A_3	k_1	k_2 (s^{-1})	k_3
2AP57 + SAM	36	64	(100)*	7.62	1.1	(0.12)*
2AP57 + SAH	22	37	41	2.9	0.3	0.04
2AP58 + SAM	24	48	31	2.8	0.6	0.13
2AP58 + SAH	18	44	38	1.3	0.2	0.04
G57-2AP58 + SAM	34	36	30	2.5	0.3	0.04
G57-2AP58 + SAH	29	27	44	2.5	0.3	0.03

()* this phase represents a decay of fluorescence corresponding to the return of the 2-AP to its canonical position in 2AP57 by $_{Pab}$TrmI. This phase was observed only with 2AP57 in the presence of SAM. The kinetics were measured at 55°C.

reached at ∼13 s (Table 2 and Figure 5B). The third kinetics phase was associated with a fluorescence increase, in contrast to 2AP57.

The fluorescence change of 2-AP in G57-2AP58-mini-RNA was also monitored under catalytic conditions, in the presence of SAM and enzyme (Figure 5C). $_{Pab}$TrmI did not methylate G57-2AP58-mini-RNA (data not shown). Therefore, the use of this mini-RNA, in which the target adenine at position 57 is replaced by another purine that is not modified, enables to set aside the influence of the methylation reaction on the base(s) recognition mechanism. Despite the fact that the presence of the amino group of guanine could have an impact on the kinetics curves, these were very similar between G57-2AP58-mini-RNA and 2AP58. The RNA binding kinetics appeared to be only slightly slower and there was no observed decrease of fluorescence intensity when a guanine is present at position 57 rather than an adenine (Table 2).

Effect of SAH on RNA binding and base recognition by $_{Pab}$TrmI

To investigate the effect of the SAH product on RNA binding, the protein was first incubated with an excess of SAH and then rapidly mixed with the various 2-AP-mini-RNAs in the stopped flow fluorimeter. The major phases of rate constants with 2AP57, 2AP58 or G57-2AP58-mini-RNA in the presence of SAH were very similar (Table 2 and Figure 5). Moreover, these kinetics were also similar to those observed with 2AP58 and G57-2AP58-mini-RNA in the presence of SAM, with no decrease of fluorescence.

Energy associated with the binding of RNA to $_{Pab}$TrmI

To determine the activation energies associated with RNA binding, base recognition and methylation of A_{57} and A_{58} by $_{Pab}$TrmI, the kinetics were recorded with 2AP57, 2AP58 or the G57-2AP58-mini-RNA in the presence of SAM at different temperatures (Supplementary Figure S5 and Supplementary Table S2). Raising the temperature enhanced the rate constants with both 2AP57 and 2AP58 without altering significantly the overall shape of the kinetics curves (Supplementary Figure S5). In the case of 2AP57, the overall amplitude of the signal diminished as the temperature increased (Supplementary Figure S5A), indicating a more pronounced temperature dependence for the last phase as evidenced by the larger activation energy (E_{a3} ∼27.7 kcal mol^{-1}) (Supplementary Figure S6 and Table S2).

Structural model of $_{Pab}$TrmI in complex with tRNA

We have recently solved the crystal structure of $_{Pab}$TrmI in free form and in complex with either SAM or SAH cofactor (16). Unfortunately and despite numerous attempts, the tRNA/TrmI complex could not be crystallized. To understand the molecular basis for the RNA recognition and binding mode employed by $_{Pab}$TrmI, we built a structural model of the enzyme/tRNA complex (Figure 6). The model was generated by rigid manual docking using the tetrameric structure of $_{Pab}$TrmI in complex with four SAM molecules (PDB code 3MB5) and a full-length maturated yeast $tRNA^{Phe}$ (PDB code 1EVV). Each monomer is organized into two domains, the N-terminal (Nt) domain and the catalytic C-terminal (Ct) domain containing the SAM binding pocket. Two pairs of monomers are associated into two dimers that combine to generate a stable tetramer. This oligomeric structure is conserved across evolution, as evidenced by several available crystal structures of $_{Pab}$TrmI orthologs (17). Interestingly, two wide and large positively charged clefts are located on the sides of the tetramer (Figure 6 and Supplementary Figure S7). Two tRNA molecules can be accommodated in these putative RNA binding pockets without clashes. In the model, the T-stem loop and acceptor stem of the tRNAs contact the catalytic domains, the anticodon region being completely oriented outside the protein. In addition, in each RNA binding site, the D-loop of the tRNA interacts with the Nt-domain of one monomer, while the double-stranded acceptor and the T-stems contact the Nt-domain of the second monomer. In this configuration, the T-loop that contains nucleotides 57 and 58 lies in

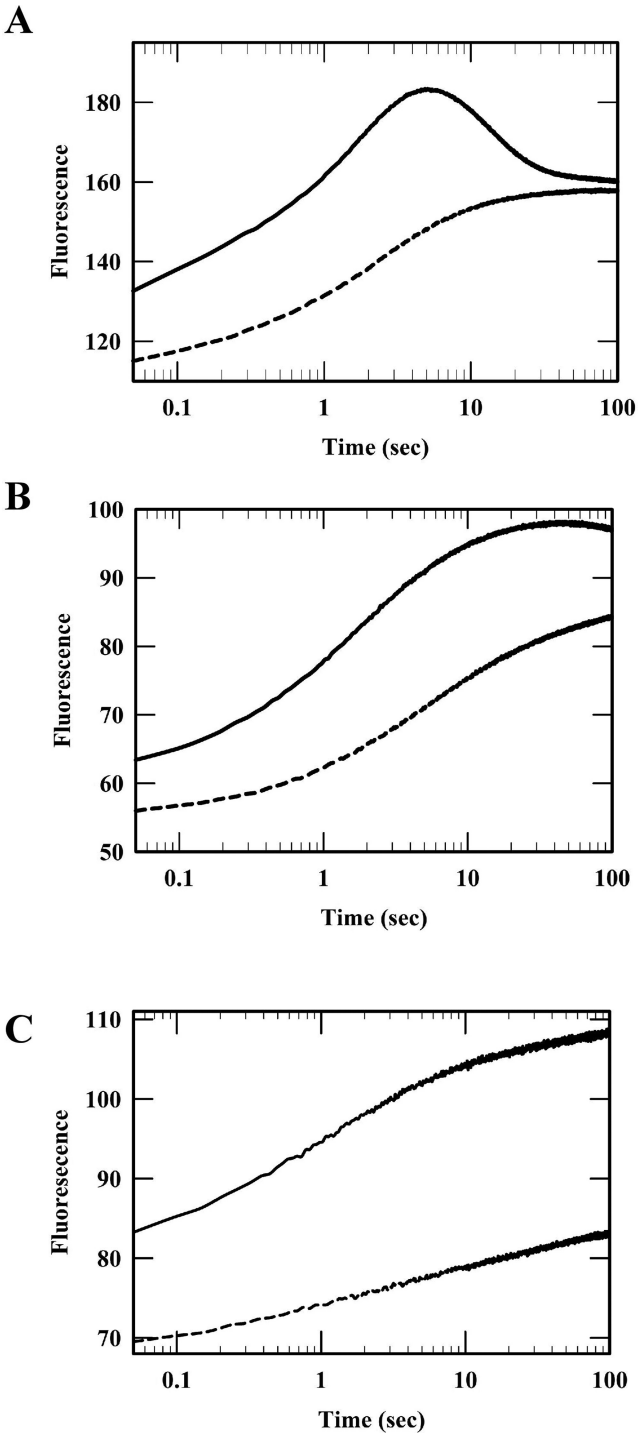

Figure 5. Base destacking kinetics of the 2-AP containing mini-RNAs by $_{Pab}$TrmI in the presence of SAM (solid lines) and SAH (dashed lines) measured by stopped-flow spectrofluorimetry at 55°C. $_{Pab}$TrmI (6 μM) and either SAM or SAH (1 mM) were pre-incubated for 10 min in one syringe, whereas the other syringe contained the 2-AP-mini-RNA with either SAM or SAH (1 mM). The reaction was started with the rapid mixing of both syringes and the total fluorescence was recorded with a WG-360 cut-off filter after exciting at 320 nm. (**A**) 2AP57. (**B**) 2AP58. (**C**) G57-2AP58-mini-RNA.

close proximity of SAM, whose methyl group is oriented toward the T-loop.

The superposition of the $_{Pab}$TrmI/tRNA model with the structures of the mono-site specific TrmI from *T. thermophilus* and *A. aeolicus* ($_{tt}$TrmI and $_{aa}$TrmI) shows that, although their catalytic domains align well, their Nt-domains are oriented differently compared to those of $_{Pab}$TrmI (Supplementary Figure S8). Keeping the same orientation of the tRNA as in the $_{pab}$TrmI complex model provokes severe clashes of the tRNA with the Nt-domains of $_{tt}$TrmI and $_{aa}$TrmI. A reorientation of the tRNA molecules and/or conformational changes of the tRNA or proteins are necessary to prevent these clashes and properly fit the macromolecule substrate into the groves of the $_{Pab}$TrmI homologs.

DISCUSSION

Our previous results indicated that the bi-specific $_{Pab}$TrmI methylates A_{58} in tRNAs containing the $A_{57}A_{58}A_{59}$ sequence only if A_{57} has already been methylated (16). The present methylation assays indicate that the 29-mer *P. abyssi* mini-tRNA^{Asp} and mini-tRNA^{Arg} constitute good substrates of $_{Pab}$TrmI as they are modified similarly to full-length tRNAs and thus they can be utilized to replace the target adenines by 2-AP. Interestingly, the enzyme did not methylate 2-AP, thereby discriminating between adenine, which contains an amino group at the C6 position, and 2-AP, in which this group is present at C2 instead of C6. Methylation kinetics under single-turnover conditions showed that A_{58} is more efficiently methylated than A_{57} when 2-AP is present at the adjacent position (57 and 58, respectively). The enzyme methylates quite efficiently A_{58} in 2AP57 probably because the introduction of 2-AP at position 57 does not much interfere with the T-loop structure nor the correct placement of A_{58} in the active site. In contrast, in 2AP58, the less efficient methylation of A57 may be due to the non-native reverse Hoogsteen base pair between U54 and 2-AP58 and/or steric hindrance caused by the NH_2 group at C2, which could hamper the optimal positioning of the nucleotides. $_{Pab}$TrmI also methylated efficiently A_{58} in a mini-RNA containing a guanine at position 57. Hence, methylation occurs at position 58 when position 57 contains a methylated adenine, an adenine derivative or guanine, whereas the methylation at position 57 strictly requires adenine 58 to proceed efficiently. This supports our previous conclusion that A57 is methylated before A58 in tRNAs containing the $A_{57}A_{58}A_{59}$ sequence (16).

The fluorescence properties of 2-AP enabled us to study the binding of RNA to $_{Pab}$TrmI. The observed increase of the 2-AP fluorescence suggests that the binding of $_{Pab}$TrmI to the 2AP-containing RNAs provokes base unstacking of the fluorescent probe itself and/or its immediate neighbors. Interestingly, this variation of fluorescence is in the same order of magnitude as that measured for placement of the target base in the active site of two RNA modifying enzymes (30–32). Accordingly, the model of $_{Pab}$TrmI in complex with tRNA clearly underlines that the enzyme has to employ a base flipping mechanism to get access to both A_{57} and A_{58}. The flipping of several bases in the vicinity of the target base by RNA modifying enzymes is a widely used mechanism, as reviewed by Li (21). The calculated appar-

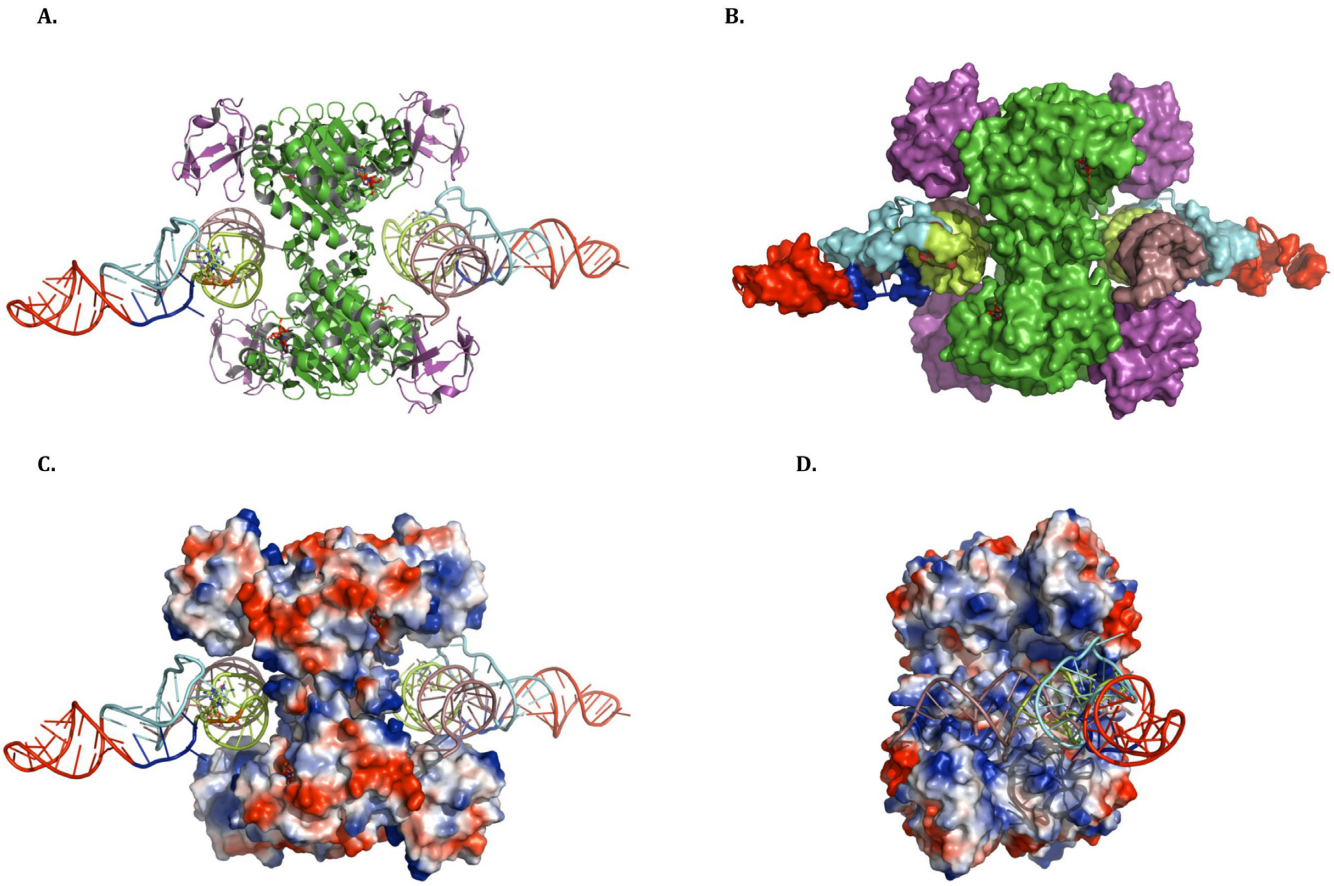

Figure 6. Model of $_{Pab}$TrmI in complex with tRNA. (**A**) Cartoon, (**B**) surface and (**C**) electrostatic representations of the enzyme/tRNA complex oriented in the same fashion. The different secondary structures of the tRNA are colored as follows: the T-psi stem loop in pale green, the D-stem loop in cyan, the anticodon stem loop in red, the variable loop in blue and the acceptor stem in salmon. The Nt and Ct domains of $_{Pab}$TrmI are in violet and green, respectively. The SAM cofactor and the target adenines are represented in red. (**D**) 90° rotation view of (C).

ent K_d values for 2AP57 and 2AP58 of 1.7 and 2.8 μM, respectively, indicate that both 2-AP-mini-RNAs are recognized by $_{Pab}$TrmI. Although the enzyme exhibits a slightly higher affinity for 2AP57, in agreement with the slightly faster binding of 2AP57 by $_{Pab}$TrmI compared to 2AP58, the position of 2-AP does not substantially alter RNA binding.

The binding kinetics of the 2-AP-containing mini-RNAs were then analyzed by stopped flow in the presence or absence of SAM or SAH. The rather complex multiphasic kinetics indicate that several molecular changes around the target bases occur, when $_{Pab}$TrmI binds to the RNAs. Similar complex kinetics have been observed for adenine glycosylase MutY (33). Indeed, stopped-flow fluorescence analysis of MutY, using a duplex oligodeoxyribonucleotide containing a uracil-2-AP base pair, revealed that the extrusion of the targeted base was followed by slower protein isomerization steps that provided an additional stabilization of the flipped out adenine in the active site, thereby facilitating excision and base repair.

In the absence of SAM, the fluorescence increase was not followed by any decrease, suggesting that $_{Pab}$TrmI recognizes both target bases in 2AP57 and 2AP58 and that 2-AP (and/or its neighbor nucleotides) may be stabilized in a destacked conformation. The enzyme is therefore able to recognize and bind RNA even in the absence of methyl donor. Remarkably, in the presence of SAM, a decrease of fluorescence occurred after the initial fluorescence increase only in the case of 2AP57. The first two increasing phases represent most likely the series of molecular events regarding the binding of the RNA and base recognition, while the last decreasing phase may be attributed to RNA dissociation after methylation of A_{58}. The absence of fluorescence decrease with 2AP58 could reflect the fact that 2-AP remains bound to the enzyme catalytic pocket or the return of 2-AP in the canonical position inside the tRNA is an extremely slow process. The similar kinetic constants shared by 2AP58 and G57-2PA58-mini-RNA, which does not undergo methylation, indicate that the observed signal of fluorescence likely originates from common events, i.e. RNA binding and base recognition in the vicinity of 2-AP. The kinetic curves for these mini-RNAs, compared with those for 2AP57, also suggest that the environment changes occurring around the 2-AP region are maintained as long as the methylation at position 58 is not achieved. Indeed, the methylation of A58 provides a gain in the stabilization energy of the U54-A58 or T54-A58 base-pairs of 6.8 kcal/mol (34), which agrees with the idea that methylation of A58

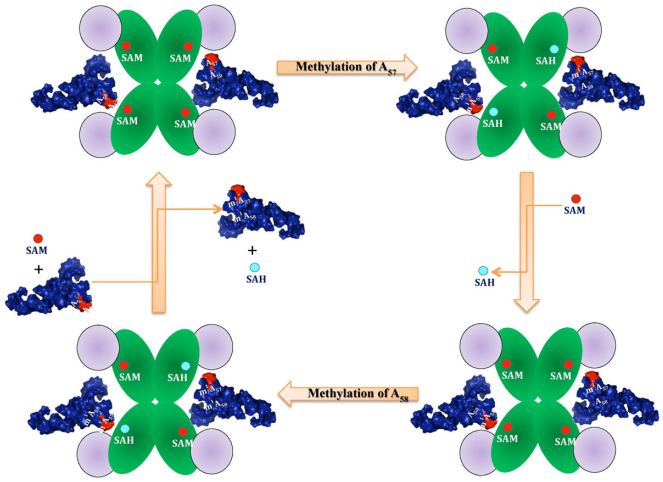

Figure 7. Proposed mechanism for the methylation of A_{57} and A_{58} by $_{Pab}$TrmI. In the presence of SAM (red circle), the tetrameric $_{Pab}$TrmI binds two tRNA molecules, recognizing specifically the T-psi stem-loop containing the region to be modified. Then, the enzyme destacks and flips out A_{57} alone or both A_{57} and A_{58} from the tRNA. The proximity of A_{57} to the SAM binding pocket enables its methylation first. The release of the first SAH molecule (blue circle), which does not promote the release of the tRNA from the enzyme, is followed by the binding of the second SAM molecule and leads to the methylation of A_{58}. The production of m^1A_{58} triggers the release of tRNA and, consequently, the enzyme, liberated from the products, becomes ready for another turnover.

will trigger the dissociation of tRNA promoted by this high driving force. We thus propose that the RNA binding dynamics are orchestrated by the methylation of adenine 58. Such a crucial role of the methylation of A_{58} is in agreement with m^1A_{58} being universally conserved in tRNAs.

The kinetics in the presence of SAH for 2AP57, 2AP58 or G57-2AP58-mini-RNA were similar to those of 2AP58 or G57-2AP58-mini-RNA in the presence of SAM. This suggests that the enzyme is capable of binding these mini-RNAs and induce a destacking of the 2-AP and/or its immediate neighbors at a similar rate, independently of the presence of SAH or SAM. Therefore, the specific recognition of the RNA by $_{Pab}$TrmI does not appear to rely on the presence of the SAM cofactor.

Finally, the temperature dependence of the kinetic constants was measured and the activation energies corresponding to the three main steps were determined by Arrhenius plots. In the case of 2AP57, the maximum of fluorescence intensity diminished as the temperature increased, indicating that the rate of the last phase assigned to the dissociation of the RNA is enhanced more than that of the first phases assigned to the recognition process, which results in a large E_{a3} value. The large E_{a1} E_{a2} and E_{a3} activation energies determined for 2AP57 may reflect the fact that the corresponding steps include the methylation of A_{58} because the E_a values for 2AP58 and the G57-2AP58-mini-RNA, in which methylation of A_{58} does not occur, are similar and relatively weak compared to those observed with 2AP57. Hence, the recognition of A_{58} together with its methylation and the flipping back of m^1A_{58} into the RNA may contribute significantly to the high activation energies observed with 2AP57.

Although the $_{Pab}$TrmI tetramer binds four SAM molecules, our model of its complex with tRNA underscores the symmetric binding of two tRNA molecules and the use of only two SAM molecules over four for catalysis. The binding of two tRNA molecules is in agreement with the MS experiments carried out with $_{tt}$TrmI (19). Our model shows that the protein interacts mainly with the T-psi stem loop and the acceptor stem of the tRNA, which is in agreement with our activity test showing that a mini-RNA substrate containing only these regions is recognized by $_{Pab}$TrmI and methylated. The model also illustrates that the flipping of both A_{57} and A_{58} is mandatory to bring both targets at a suitable distance for methyl transfer. In particular, flexible loops of the Nt-domain that are in close contact with the T-loop could be determinant to untighten the tertiary interactions at the elbow of the tRNA (intersecting region between the D- and T-loops) and promote base flipping. Except base flipping, no dramatic conformational change of the tRNA appears necessary for the reaction to occur, as observed for most RNA-modifying enzymes. In particular, *T. thermophilus* dihydrouridine synthase, which modifies U20 in the D-loop of tRNA, does not require extensive conformational changes in the tRNA to access its target base because the canonical D-loop/T-loop interaction was maintained in the crystal structure of the complex (35). The larger RNA binding pocket of $_{Pab}$TrmI compared to that of other mono-site-specific TrmIs (17) may enable much more flexibility in the binding of the tRNA and would allow the enzyme to position A57 or A58 for methylation without serious steric hindrance. In addition, the rather large solvent accessibility of the SAM binding pocket, even in the presence of tRNA, agrees with the fact that the first SAH molecule could dissociate after methylation of the first adenine and be replaced by the second SAM molecule without provoking tRNA dissociation, thereby enabling the consecutive methylation of the second adenine. This scenario is supported by the comparison of the crystal structures of $_{Pab}$TrmI alone, in complex with SAH or SAM, which does not highlight noticeable conformational changes (16). A general mechanism for the double methylation of tRNA by $_{Pab}$TrmI can thus be proposed (Figure 7).

Multi-site RNA modifying enzymes may share a similar sequential dynamical process and the same method that uses oligonucleotides containing 2-AP at the target positions may be implemented for the investigation of the RNA conformational changes occurring during catalysis by these enzymes.

SUPPLEMENTARY DATA

Supplementary Data are available at NAR Online.

FUNDING

CNRS. Funding for open access charge: French State Program 'Investissements d'Avenir' [LABEX DYNAMO ANR-11-LABX-0011].
Conflict of interest statement. None declared.

REFERENCES

1. Gustilo,E.M., Vendeix,F.A. and Agris,P.F. (2008) tRNA's modifications bring order to gene expression. *Curr. Opin. Microbiol.*, **11**, 134–140.
2. Motorin,Y. and Helm,M. (2010) tRNA stabilization by modified nucleotides. *Biochemistry*, **49**, 4934–4944.
3. El Yacoubi,B., Bailly,M. and de Crecy-Lagard,V. (2012) Biosynthesis and function of posttranscriptional modifications of transfer RNAs. *Annu. Rev. Genet.*, **46**, 69–95.
4. Agris,P.F. (2004) Decoding the genome: a modified view. *Nucleic Acids Res.*, **32**, 223–238.
5. Awai,T., Kimura,S., Tomikawa,C., Ochi,A., Ihsanawati,, Bessho,Y., Yokoyama,S., Ohno,S., Nishikawa,K., Yokogawa,T. *et al.* (2009) *Aquifex aeolicus* tRNA (N2,N2-guanine)-dimethyltransferase (Trm1) catalyzes transfer of methyl groups not only to guanine 26 but also to guanine 27 in tRNA. *J. Biol. Chem.*, **284**, 20467–20478.
6. Awai,T., Ochi,A., Ihsanawati,, Sengoku,T., Hirata,A., Bessho,Y., Yokoyama,S. and Hori,H. (2011) Substrate tRNA recognition mechanism of a multisite-specific tRNA methyltransferase, *Aquifex aeolicus* Trm1, based on the X-ray crystal structure. *J. Biol. Chem.*, **286**, 35236–35246.
7. Hur,S. and Stroud,R.M. (2007) How U38, 39, and 40 of many tRNAs become the targets for pseudouridylation by TruA. *Mol. Cell*, **26**, 189–203.
8. Poldermans,B., Roza,L. and Van Knippenberg,P.H. (1979) Studies on the function of two adjacent N6,N6-dimethyladenosines near the 3′ end of 16 S ribosomal RNA of *Escherichia coli*. III. Purification and properties of the methylating enzyme and methylase-30 S interactions. *J. Biol. Chem.*, **254**, 9094–9100.
9. Cunningham,P.R., Weitzmann,C.J., Nurse,K., Masurel,R., Van Knippenberg,P.H. and Ofengand,J. (1990) Site-specific mutation of the conserved m6(2)A m6(2)A residues of *E. coli* 16S ribosomal RNA. Effects on ribosome function and activity of the ksgA methyltransferase. *Biochim. Biophys. Acta*, **1050**, 18–26.
10. Tu,C., Tropea,J.E., Austin,B.P., Court,D.L., Waugh,D.S. and Ji,X. (2009) Structural basis for binding of RNA and cofactor by a KsgA methyltransferase. *Structure*, **17**, 374–385.
11. Roovers,M., Wouters,J., Bujnicki,J.M., Tricot,C., Stalon,V., Grosjean,H. and Droogmans,L. (2004) A primordial RNA modification enzyme: the case of tRNA (m^1A) methyltransferase. *Nucleic Acids Res.*, **32**, 465–476.
12. Anderson,J., Phan,L., Cuesta,R., Carlson,B.A., Pak,M., Asano,K., Bjork,G.R., Tamame,M. and Hinnebusch,A.G. (1998) The essential Gcd10p-Gcd14p nuclear complex is required for 1-methyladenosine modification and maturation of initiator methionyl-tRNA. *Genes Dev.*, **12**, 3650–3662.
13. Droogmans,L., Roovers,M., Bujnicki,J.M., Tricot,C., Hartsch,T., Stalon,V. and Grosjean,H. (2003) Cloning and characterization of tRNA (m^1A58) methyltransferase (TrmI) from *Thermus thermophilus* HB27, a protein required for cell growth at extreme temperatures. *Nucleic Acids Res.*, **31**, 2148–2156.
14. Grosjean,H., Constantinesco,F., Foiret,D. and Benachenhou,N. (1995) A novel enzymatic pathway leading to 1-methylinosine modification in *Haloferax volcanii* tRNA. *Nucleic Acids Res.*, **23**, 4312–4319.
15. Constantinesco,F., Motorin,Y. and Grosjean,H. (1999) Transfer RNA modification enzymes from *Pyrococcus furiosus*: detection of the enzymatic activities in vitro. *Nucleic Acids Res.*, **27**, 1308–1315.
16. Guelorget,A., Roovers,M., Guérineau,V., Barbey,C., Li,X. and Golinelli-Pimpaneau,B. (2010) Insights into the hyperthermostability and unusual region-specificity of archaeal *Pyrococcus abyssi* tRNA m1A57/58 methyltransferase. *Nucleic Acids Res.*, **38**, 6206–6218.
17. Guelorget,A., Barraud,P., Tisné,C. and Golinelli-Pimpaneau,B. (2011) Structural comparison of tRNA m(1)A58 methyltransferases revealed different molecular strategies to maintain their oligomeric architecture under extreme conditions. *BMC Struct. Biol.*, **11**, 48.
18. Kuratani,M., Yanagisawa,T., Ishii,R., Matsuno,M., Si,S.Y., Katsura,K., Ushikoshi-Nakayama,R., Shibata,R., Shirouzu,M., Bessho,Y. *et al.* (2014) Crystal structure of tRNA m(1)A58 methyltransferase TrmI from *Aquifex aeolicus* in complex with S-adenosyl-L-methionine. *J. Struct. Funct. Genomics*, **15**, 173–180.
19. Barraud,P., Golinelli-Pimpaneau,B., Atmanène,C., Sanglier,S., van Dorsselaer,A., Droogmans,L., Dardel,F. and Tisné,C. (2008) Crystal structure of *Thermus thermophilus* tRNA m^1A58 methyltransferase and biophysical characterization of its interaction with tRNA. *J. Mol. Biol.*, **377**, 535–550.
20. Ishitani,R., Yokoyama,S. and Nureki,O. (2008) Structure, dynamics, and function of RNA modification enzymes. *Curr. Opin. Struct. Biol.*, **18**, 330–339.
21. Li,H. (2007) Complexes of tRNA and maturation enzymes: shaping up for translation. *Curr. Opin. Struct. Biol.*, **17**, 293–301.
22. Rachofsky,E.L., Osman,R. and Ross,J.B. (2001) Probing structure and dynamics of DNA with 2-aminopurine: effects of local environment on fluorescence. *Biochemistry*, **40**, 946–956.
23. Holz,B., Klimasauskas,S., Serva,S. and Weinhold,E. (1998) 2-Aminopurine as a fluorescent probe for DNA base flipping by methyltransferases. *Nucleic Acids Res.*, **26**, 1076–1083.
24. Lenz,T., Bonnist,E.Y., Pljevaljcic,G., Neely,R.K., Dryden,D.T., Scheidig,A.J., Jones,A.C. and Weinhold,E. (2007) 2-Aminopurine flipped into the active site of the adenine-specific DNA methyltransferase M.TaqI: crystal structures and time-resolved fluorescence. *J. Am. Chem. Soc.*, **129**, 6240–6248.
25. Lang,K., Rieder,R. and Micura,R. (2007) Ligand-induced folding of the thiM TPP riboswitch investigated by a structure-based fluorescence spectroscopic approach. *Nucleic Acids Res.*, **35**, 5370–5378.
26. Hall,K.B. (2009) 2-aminopurine as a probe of RNA conformational transitions. *Methods Enzymol.*, **469**, 269–285.
27. Sarkar,K., Nguyen,D.A. and Gruebele,M. (2010) Loop and stem dynamics during RNA hairpin folding and unfolding. *RNA*, **16**, 2427–2434.
28. Souliere,M.F., Haller,A., Rieder,R. and Micura,R. (2011) A powerful approach for the selection of 2-aminopurine substitution sites to investigate RNA folding. *J. Am. Chem. Soc.*, **133**, 16161–16167.
29. Douthwaite,S. and Kirpekar,F. (2007) Identifying modifications in RNA by MALDI mass spectrometry. *Methods Enzymol.*, **425**, 1–20.
30. Watts,J.M., Gabruzsk,J. and Holmes,W.M. (2005) Ligand-mediated anticodon conformational changes occur during tRNA methylation by a TrmD methyltransferase. *Biochemistry*, **44**, 6629–6639.
31. Liang,B., Xue,S., Terns,R.M., Terns,M.P. and Li,H. (2007) Substrate RNA positioning in the archaeal H/ACA ribonucleoprotein complex. *Nat. Struct. Mol. Biol.*, **14**, 1189–1195.
32. Liang,B., Kahen,E.J., Calvin,K., Zhou,J., Blanco,M. and Li,H. (2008) Long-distance placement of substrate RNA by H/ACA proteins. *RNA*, **14**, 2086–2094.
33. Wong,I., Lundquist,A.J., Bernards,A.S. and Mosbaugh,D.W. (2002) Presteady-state analysis of a single catalytic turnover by *Escherichia coli* uracil-DNA glycosylase reveals a 'pinch-pull-push' mechanism. *J. Biol. Chem.*, **277**, 19424–19432.
34. Oliva,R., Cavallo,L. and Tramontano,A. (2006) Accurate energies of hydrogen bonded nucleic acid base pairs and triplets in tRNA tertiary interactions. *Nucleic Acids Res.*, **34**, 865–879.
35. Yu,F., Tanaka,Y., Yamashita,K., Suzuki,T., Nakamura,A., Hirano,N., Suzuki,T., Yao,M. and Tanaka,I. (2011) Molecular basis of dihydrouridine formation on tRNA. *Proc. Natl Acad. Sci. U.S.A.*, **108**, 19593–19598.